4372 *Chem. Mater.* **2010,** *22,* 4372–4378
DOI:10.1021/cm100442x

CHEMISTRY OF MATERIALS
Article

Quantum Dots with Multivalent and Compact Polymer Coatings for Efficient Fluorescence Resonance Energy Transfer and Self-Assembled Biotagging

Hongwei Duan,*,† Min Kuang,*,‡ and Y. Andrew Wang‡

†*School of Chemical and Biomedical Engineering, Nanyang Technological University, 70 Nanyang Drive, Singapore 637457, and* ‡*Ocean Nanotech, 2143 Worth Lane, Springdale, Arkansas 72764*

Received February 11, 2010. Revised Manuscript Received May 24, 2010

Multicolor quantum dot (QD) probes with compact sizes, excellent colloidal stability, and high quantum yields were developed by using a new class of multivalent polymer ligands based on poly(maleic anhydride) homopolymer. These size-minimized QDs allow facile construct of bioconjugated QDs through metal-affinity chelating between polyhistidine (His) tags of recombinant proteins and QD surfaces. Our results have shown that fluorescent protein, for example, mCherry with His-tag, is able to assemble on the QD surface and give rise to highly efficient fluorescence resonance energy transfer (FRET) between the QD donor and the fluorescent protein acceptor. Our results suggest that using this new class of compact QD probes leads to significant enhancement of FRET efficiency in comparison with the bulky amphiphilic polymer encapsulated QDs. We have also found that self-assembled QD probes can be successfully used for immunofluorescence cell staining, indicating that this self-assembled biotagging strategy is both versatile and robust in nature.

Introduction

Semiconductor quantum dots (QDs) have shown promise for biomedical applications ranging from ultrasensitive analysis, single molecular detection to cellular and in vivo imaging.[1−5] Enormous research efforts have been stimulated by their unique optical and spectroscopic properties that are not available from conventional organic dyes and fluorescent proteins. Particularly, the superior brightness and photostability of QDs are of great importance for continuous tracking of the molecular process;[6−8] their narrow and size-tunable emission spectra and broad excitation profiles have offered new possibilities in multiplexed detection and optical imaging.[9] While tremendous progress has been made in chemically synthesizing QDs with improved and better controlled optical properties, a great deal of attention has been paid to rationally designing surface coatings of QDs for biological applications, because increasing evidence shows that surface coatings not only provide water-solubility, colloidal stability, and surface functionalities for bioconjugation but also play important roles in controlling the interaction of QDs with biomolecules and cell membrane, their intracellular pathway, and even their in vivo biodistribution.[1,5]

The majority of QDs currently used for biological studies are encapsulated with amphiphilic copolymers, which leads to a significant size increase compared to bare QDs due to the presence of a hydrophobic layer formed by QD capping ligands and hydrophobic moiety of the amphiphilic polymers.[10−12] Although the amphiphilic copolymer coating provides a highly stable platform for surface functionalization, the bulky size of these QDs is especially detrimental to fluorescence resonance energy transfer (FRET) based assays,[3] which are highly sensitive to donor−acceptor distance and imaging of intracellular processes in which bulky sizes lead to limited diffusion of QDs inside cytoplasm and could compromise the molecular binding as a result.[13] Therefore, it is of considerable

*Corresponding authors. E-mail: hduan@ntu.edu.sg, mkuang@oceannanotech.com.

(1) Michalet, X.; Pinaud, F. F.; Bentolila, L. A.; Tsay, J. M.; Doose, S.; Li, J. J.; Sundaresan, G.; Wu, A. M.; Gambhie, S. S.; Weiss, S. *Science* **2005**, *307*, 538–544.
(2) Alivisatos, A. P.; Gu, W. W.; Larabell, C. *Ann. Rev. Biomed. Eng.* **2005**, *7*, 55–76.
(3) Medintz, I. L.; Tetsuo, U.; Goldman, E. R.; Mattoussi, H. *Nat. Mater.* **2005**, *4*, 435–446.
(4) Klostranec, J. M.; Chan, W. C. W. *Adv. Mater.* **2006**, *18*, 1953–1964.
(5) Smith, A. M.; Duan, H. W.; Mohs, A. M.; Nie, S. M. *Adv. Drug Delivery Rev.* **2008**, *60*, 1226–1240.
(6) Courty, S.; Luccardini, C.; Bellaiche, Y.; Cappelo, G.; Dahan, M. *Nano Lett.* **2006**, *6*, 1491–1495.
(7) Ruan, G.; Agrawal, A.; Marcus, A. I.; Nie, S. M. *J. Am. Chem. Soc.* **2007**, *129*, 14759–14766.
(8) Howarth, M.; Liu, W. H.; Puthenveetil, S.; Zheng, Y.; Marshall, L. F.; Schmidt, M. M.; Wittrup, K. D.; Bawendi, M. G.; Ting, A. Y. *Nat. Methods* **2008**, *5*, 397–399.
(9) Yezhelyev, M.; Al-Hajj, A.; Morris, C.; Marcus, A. I.; Liu, T. Q.; Lewis, M.; Cohen, C.; Zrazhevskiy, P.; Simons, J. W.; Nie, S. M.; Gao, X. H.; O'Regan, R. M. *Adv. Mater.* **2007**, *19*, 3146–3151.
(10) Wu, X. Y.; Liu, H. J.; Liu, J. Q.; Haley, K. N.; Treadway, J. A.; Larson, J. P.; Ge, N. F.; Peale, F.; Bruchez, M. P. *Nat. Biotechnol.* **2003**, *21*, 41–46.
(11) Pellegrino, T.; Manna, L.; Kudera, S.; Liedl, T.; Koktysh, D.; Rogach, A. L.; Keller, S.; Rädler, J.; Natile, G.; Parak, W. J. *Nano Lett.* **2004**, *4*, 703–707.
(12) Yu, W. W.; Chang, E.; Falkner, J. C.; Zhang, J. Y.; Al-Somali, A. M.; Sayes, C. M.; Johns, J.; Drezek, R.; Colvin, V. L. *J. Am. Chem. Soc.* **2007**, *129*, 2871–2879.
(13) Lees, E. E.; Nguyen, T. L.; Clayton, A. H. A.; Mulvaney, P. *ACS Nano* **2009**, *5*, 1121–1128.

Published on Web 07/13/2010

interest to develop compact surface coating for QDs while maintaining their quantum yield (QY) and photo/colloidal stability.[13−23] Major efforts have focused on minimizing the sizes of QDs by replacing the capping ligand with long alkyl chains through ligand exchange reactions.[15−23] The use of small hydrophilic capping ligands can substantially reduce the thickness of surface coatings; however, the QDs obtained typically show lower long-term colloidal stability and reduced brightness in comparison with the amphiphilic polymer coated ones.[15−18] To address the stability problem of small molecule coated QDs, a number of multidentate polymer ligands have also been developed to minimize hydrodynamic sizes of QDs.[19−23] However, until very recently, the related studies have focused on the impact of polymer coatings on the optical and colloidal properties, and uses of the QDs for imaging and sensing applications have not been tested.[24]

Here we present the development of compact QD probes based on the use of a new type of multivalent polymer ligand with multiple thiol pendant groups. QDs capped with this novel multivalent ligand based on poly(maleic anhydride) homopolymer not only exhibit a combination of interesting properties such as small hydrodynamic sizes, long-term stability, high quantum yield, and resistance to photobleaching, they also allow facile construct of bioconjugated QDs through metal-affinity chelating between polyhistidine (His) tags of recombinant proteins and QD surfaces. Our results have shown that a model protein, for example, mCherry fluorescent protein with His-tag, is able to assemble on the QD surface and give rise to highly efficient FRET between the QD donor and the fluorescent protein acceptor. FRET is a process in which a donor in the excited state nonradiatively transfers energy to a proximal ground-state acceptor through a long-range dipole−dipole coupling; it has become a powerful technique to investigate molecular-level changes in the range of 1−10 nm by taking advantage of the drastic change of FRET efficiency due to variations in the donor−acceptor distance.[25,26] The current study demonstrates the importance of using this new class of compact QDs for FRET-based assays by comparing it with amphiphilic polymer coated QDs in terms of FRET efficiency. Our results in this model system suggest that the use of the compact QDs leads to significantly higher FRET efficiency than the traditional QDs encapsulated with amphiphilic copolymers. Furthermore, we have also found that self-assembled QD probes can be successfully used for immunofluorescence cell staining, indicating that this self-assembled biotagging strategy is both versatile and robust in nature.

Experimental Section

Materials. Cadmium oxide (99.99%), sulfur (99.98%, powder), trioctylphosphine oxide (TOPO, 90%), 1-octadecene (ODE, 90%), oleic acid (OA, 90%), nickel chloride, N_α,N_α-bis(carboxymethyl)-L-lysine hydrate, cysteamine, 4-(dimethylamino)pyridine (DMAP), and poly(maleic anhydride-*alt*-octadecene) (PMO, MW = 30 000−50 000 Da) were purchased from Aldrich. Selenium powder, zinc oxide (99.99% powder), tributylphosphine (TBP), and octadecylamine (ODA) were purchased from Alfa. Octodecylphosphonic acid (ODPA) and poly(maleic anhydride) (MW = 5000 Da) were from PolyScience. NH_2-dPEG$_8$-OH (MW = 370 Da) was obtained from Quanta Biodesign.

QD Synthesis. CdSe/ZnS (green and yellow) and CdSe/CdS/ZnS (orange and red) QDs were synthesized based on previous reports.[27] A typical synthesis of 620 nm CdSe/CdS/ZnS is summarized below.

CdSe Core Synthesis. The mixture of 2 mmol of CdO, 8 mmol of stearic acid, and 20 g of ODE in a 250 mL three-neck flask was heated to about 250 °C to obtain a colorless clear solution. After this solution was cooled to room temperature, ODA (15 g) and 5 g of TOPO were added into the flask. Under argon flow, this system was reheated to 280 °C. At this temperature, a selenium solution made by dissolving 16 mmol of Se in 6 g of TBP was quickly injected. The growth temperature was then reduced to 250 °C for 5 min. The emission peak of the CdSe nanocrystals should be around 560−570 nm. The reaction mixture was cooled to room temperature, and nanocrystals were separated from side products and unreacted precursors by extraction.

CdSe/CdS/ZnS Core−Shell QD Synthesis. CdSe nanocrystals (3.8 μmol of particles) were mixed with 100 g of ODE and 30 g of ODA in a three-neck flask. The mixture was heated to 220 °C in argon atmosphere for further growth. The 9 mL of Cd and 9 mL of S precursors were injected to the flask for the shell layer growth in the order of Cd−S at the interval of 10 min for each injection. After the reaction temperature was increased to 240 °C, Zn, Cd, and S precursors were added alternatively into the flask in the order and amount of Zn (4.5 mL)−Cd (4.5 mL)−S (9 mL)−Zn (9 mL)−S (9 mL)−Zn (9 mL). The reaction mixture was allowed to cool to room temperature and precipitate by acetone and followed by hexane extraction and precipitation with acetone or methanol.

Multivalent Ligand Synthesis. To synthesize the multivalent ligand, 1.0 g of poly(maleic anhydride) (MW = 5000 Da) was dissolved in 5 mL of DMSO containing 20 mg of DMAP, and 320 mg of cysteamine was added as solid. With the reaction going on at room temperature, the cysteamine solid gradually dissolved within 2 h. After another 4 h, the product, named as

(14) Smith, A. M.; Nie, S. M. *Nat. Biotechnol.* **2009**, *27*, 732–733.
(15) Smith, A. M.; Duan, H. W.; Rhyner, M. N.; Ruan, G.; Nie, S. M. *Phys. Chem. Chem. Phys.* **2006**, *8*, 3895–3903.
(16) Uyeda, H. T.; Medintz, I. L.; Jaiswal, J. K.; Simon, S. M.; Mattoussi, H. *J. Am. Chem. Soc.* **2005**, *127*, 3870–3878.
(17) Gao, M. Y.; Kirstein, S.; Mohwald, H.; Rogach, A. L.; Kornowshi, A.; Eychmuller, A.; Weller, H. *J. Phys. Chem. B* **1998**, *102*, 8360–8363.
(18) Lu, H. C.; Schöps, O.; Woggon, U.; Niemeyer, C. M. *J. Am. Chem. Soc.* **2008**, *130*, 4815–4827.
(19) Kim, S. W.; Kim, S.; Tracy, J. B.; Jasanoff, A.; Bawendi, M. G. *J. Am. Chem. Soc.* **2004**, *127*, 4556–4557.
(20) Wang, X. S.; Dykstra, T. E.; Salcador, M. R.; Manners, I.; Scholes, G. D.; Winnik, M. A. *J. Am. Chem. Soc.* **2004**, *127*, 7784–7785.
(21) Zhang, T. R.; Ge, J. P.; Hu, Y. X.; Yin, Y. D. *Nano Lett.* **2007**, *10*, 3203–3207.
(22) Smith, A. M.; Nie, S. M. *J. Am. Chem. Soc.* **2008**, *130*, 11278–11279.
(23) Yildiz, I.; McCaughan, B.; Cruickshank, S. F.; Callan, J. F.; Raymo, F. M. *Langmuir* **2009**, *25*, 7090–7096.
(24) Liu, W. H.; Greytak, A. B.; Lee, J. M.; Wong, C. R.; Park, J. N.; Marshall, L. F.; Jiang, W.; Curtin, P. N.; Ting, A. Y.; Nocera, D. G.; Fukumura, D.; Jain, R. K.; Bawendi, M. G. *J. Am. Chem. Soc.* **2010**, *132*, 472–483.
(25) Jares-Erijman, E. A.; Jovin, T. M. *Nat. Biotechnol.* **2003**, *11*, 1387–1395.
(26) Sapsford, K. E.; Berti, L.; Medintz, I. L. *Angew. Chem., Int. Ed.* **2006**, *45*, 4562–4588.
(27) Sun, Q. J.; Wang, Y. A.; Li, L. S.; Wang, D. Y.; Zhu, T.; Xu, J.; Yang, C. H.; Li, Y. F. *Nat. Photonics* **2007**, *1*, 717–722.
(28) Duan, H. W.; Kuang, M.; Wang, X. X.; Wang, Y. A.; Mao, H.; Nie, S. M. *J. Phys. Chem. C* **2008**, *112*, 8127–8131.

PMAS, was purified by precipitation in water followed by lyophilization. Note that all the reaction mixture and solvents used in purification were purged with nitrogen to avoid oxidation of thiol groups. Elemental analysis confirmed that cysteamine quantitatively reacted with poly(maleic anhydride). The obtained product has excellent solubility in DMSO and is also soluble in the mixture of DMSO and chloroform (v:v, 1:1).

Ligand Exchange. In a typical procedure, QD in chloroform was slowly added into PMAS solution in the mixture of chloroform and DMSO (v:v, 1:2), forming a clear solution. Both of the two components were deaerated with nitrogen for 30 min before being mixed, and the inert atmosphere was kept throughout the ligand exchange reaction. The reaction mixture was heated at 50 °C for about 2 h, and then chloroform was removed by rotary evaporation. After additional 4 h of heating at 90 °C, the obtained clear solution was cooled down, and the PMAS coated QDs were collected by centrifugation at 6000 g for 10 min after being precipitated in a chloroform and hexane mixture (1:1). The recovered QD was washed three times with acetone and treated with heterobifunctional polyethylene glycol (PEG) with primary amine and hydroxyl terminal groups in 50 mM pH 8.5 borate buffer; the solid gradually dissolved within 30 min, and free unbound PMAS ligands were removed by an ultrafiltration device with a cutoff of 50 kDa. Quantum yields of the QDs were measured by an integrating sphere (Ocean Optics).

QDs Coated with Amphiphilic Copolymers Containing the Complex of Ni^{2+} and Nitrilotriacetic Acid (Ni-NTA). QDs coated with the amphiphilic copolymer of maleic anhydride and octadecene (PMO) and PMO with Ni-NTA functionality (PMO-Ni-NTA) were prepared following a standard protocol we developed previously.[12,28] The Ni-NTA functionality was introduced by reacting the complex of N_α,N_α-bis(carboxymethyl)-L-lysine hydrate and Ni^{2+} with PMO in the presence of DMAP. In the current study, about 10−15% of the anhydride group was modified. To coat QDs, the polymer was mixed with QDs at a molar ratio of 1000:1 in chloroform, and the solvent was removed under vacuum after the solution was stirred for 8 h. The dried film was then dissolved in pH 8.5 borate buffer under ultrasonication, and the excess (free) polymer was removed by ultracentrifugation at 80k rpm for 45 min. To graft PEG on QDs coated PMO, 1 mL of QDs (1.0 μM) in 50 mM pH 7.0 borate buffer was mixed with mPEG-NH_2 (MW = 5000 Da) at a molar ratio of 1:1000. 60 μL *N*-(3-dimethylaminopropyl)-*N*′-ethylcarbodiimide hydrochloride (EDAC, 10 mg/mL) solution was added into the solution above to catalyze the coupling of primary amines of PEG and carboxylic acid groups on QD surfaces. The reaction was left at room temperature for 6 h before being purified by ultracentrifugation.

Self-Assembly of His-tag Protein onto QDs. QDs were mixed with His-tag proteins in 10 mM pH 8.5 borate buffer at predetermined molar ratios, and fluorescence spectra (400 nm excitation) were collected after incubation for 2 h at room temperature. For electrophoresis experiments, samples were loaded on 1% agarose gels supplemented with 1 X TAE buffer and run at 100 V for 30 min at room temperature. Fluorescent images were collected using 365 nm excitation and emission filters for SYBR-Green and ethidium bromide (EtBr).

Fluorescence Staining of Fixed Cells. Prior to QD staining, fixed MDA-MB-231 cells were labeled with philloidin-XX-Biotin (Molecular Probes) using a standard protocol of the product. QD@PMAS tagged with streptavidin (His-tag, Abcam) was dissolved in 20 mM Tris-HCl (pH 7.5, 0.3% Triton X-100, 1% BSA) and was incubated with the fixed cells for 20 min. Afterward, the slide was washed with PBS, mounted with antifading medium, and finally covered with a coverslip. The fluorescence image was recorded using an inverted epifluorescence microscope (Zeiss Axiovert 200M) with a 40× objective.

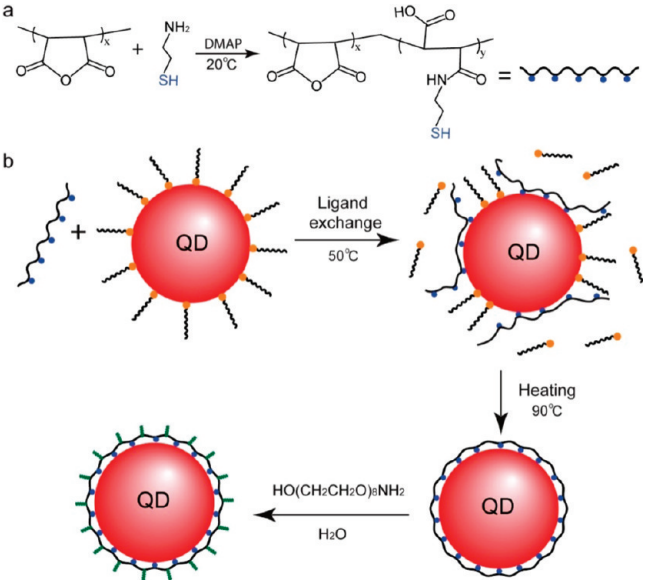

Figure 1. Schematic illustration of the synthesis of the multivalent PMAS ligands (a) and the procedure to prepare PMAS coated QDs (b).

Analysis of Energy Transfer Data. The Förster distance (R_0), which is defined as the distance between donor and acceptor that yields an energy transfer efficiency (E) of 50%, is calculated based on eq 1, using software (Photochemcad) developed by Du et al.[29] κ^2 shows the donor−acceptor transition dipole orientation, and it has a value of 2/3 for randomly oriented dipoles, which is also valid for the current system. n is the refractive index of the medium, which is 1.4 here for aqueous medium. Q_D is the quantum yield of the donor in the absence of the acceptor. $J(\lambda)$ is the overlap integral of the spectra of the donor emission and the acceptor absorption, and can be calculated by the software mentioned above. For 550 nm QD and mCherry, $J(\lambda)$ has a value of 3.5×10^{-13} cm^6·mmol^{-1}. The experimental FRET efficiency E was obtained using eq 2, in which F_D is the fluorescence of the donor in the absence of the acceptor and F_{DA} is the fluorescence of the donor in the presence of the donor. The actual donor−acceptor distance can be derived using eq 3, where n is the average number of acceptors linked to the donor and r is the distance between the donor and the acceptor, based on R_0 and E obtained.

$$R_0 = [9.78 \times 10^3 \kappa^2 n^{-4} Q_D J(\lambda)]^{1/6} \text{ (in Å)} \quad (1)$$

$$E(n,r) = \frac{(F_D - F_{DA})}{F_D} \quad (2)$$

$$E(n,r) = \frac{n}{n + \left(\frac{r}{R_0}\right)^6} \quad (3)$$

Results and Discussion

Synthesis of Compact QD Probes. As illustrated in Figure 1a, the multivalent polymer ligand PMAS with thiol

(29) Du, H.; Fuh, R. C. A.; Li, J. Z.; Corkan, L. A.; Lindsey, J. S. *Photochem. Photobiol.* **1998**, *68*, 141–142.

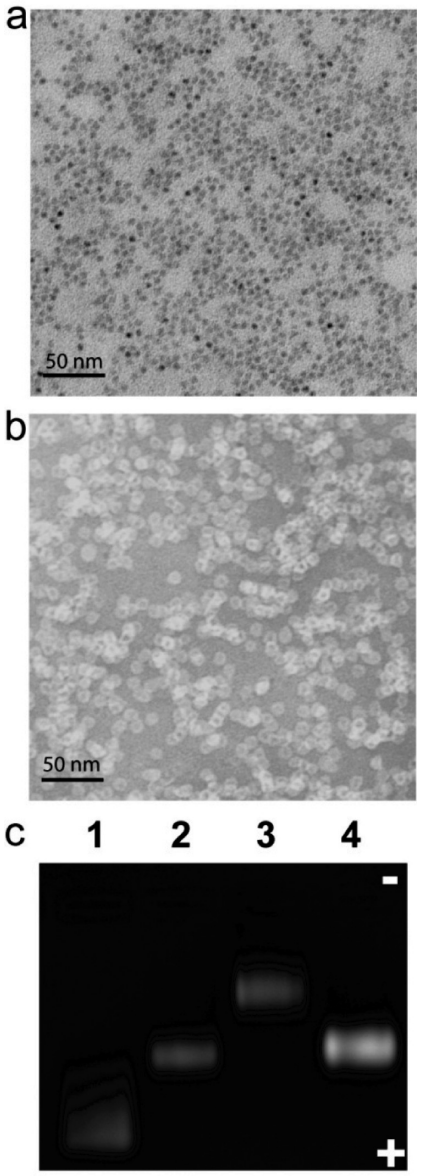

Figure 2. Transmission electron micrographs of negatively stained PMAS (a) and PMO (b) coated 610 nm QD (CdSe/CdS/ZnS). (c) Electrophoretic characterization of QDs with various types of surface coatings: PMAS (lane 1), PMO with NTA fucntionality (lane 2), PMO with PEG grafts (lane 3), and PMO (lane 4).

pendant groups was synthesized by reacting poly(maleic anhydride) (MW = 5000 Da) with cysteamine. The high reactivity of anhydride with primary amines facilitated the quantitatively controlled reaction. In an optimized structure, about 40% of the maleic anhydride groups were chemically modified. This composition not only led to strong binding affinity of PMAS (on average 20 thiol groups per polymer chain) to QD surfaces but also maintains its good solubility in a mixture of dimethyl sulfoxide (DMSO) and chloroform. The original core−shell QDs (CdSe/ZnS or CdSe/CdS/ZnS) with hydrophobic ligands are also dispersible in the mixture but not in pure highly polar solvents including DMSO. This common solubility of the PMAS ligand and QDs in the mixture offers possibilities for one-step ligand exchange of QDs and PMAS ligands in this solvent system. In comparison, Smith et al. showed that the use of ligands based on

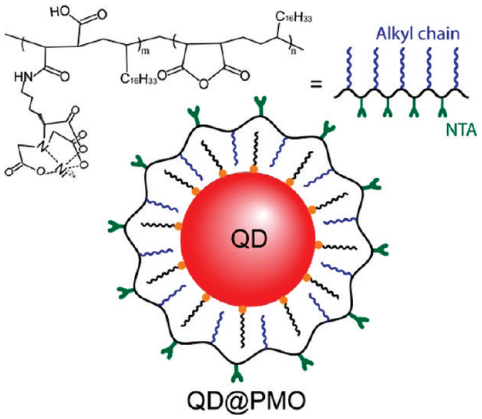

Figure 3. Schematic illustration of surface coating chemistry of amphiphilic PMO copolymer coated QDs with Ni-NTA functionality.

Table 1. Hydrodynamic Diameters and Structural Parameters of the 4.2 and 6.0 nm QDs Coated with the PMAS Ligands and the PMO Amphiphilic Copolymer

QD sizes (nm)	surface coatings	hydrodynamic diameter (nm)	coating thickness (nm)
4.2	PMAS	7.3 ± 2.4	1.6
4.2	PMO	11.2 ± 2.7	3.5
6.0	PMAS	9.0 ± 1.9	1.5
6.0	PMO	14.0 ± 2.3	4.0

poly(acrylic acid) (PAA), which is only soluble in polar solvents, has to go through two ligand exchange reactions, using small molecular ligands, that is, thioglycerol coated QDs as an intermediate state to provide miscibility between QDs and PAA-based ligands in DMSO.[22] Obviously, the additional ligand exchange necessitates a sophisticated optimization of the chemical composition of the PAA-based ligands to maintain the optical properties of QDs.

In this study, the coating process (Figure 1b) is completed by the ligand exchange under a two-stage heating at 50 and 90 °C and a following reaction with a heterobifunctional polyethylene glycol (PEG, MW = 370 Da) with primary amine and hydroxyl terminal groups to obtain water-soluble QDs. An interesting finding is that the initial 2 h heating at 50 °C led to QDs soluble in DMSO; however, compact QDs with long-term stability can only be produced after additional heating at 90 °C for 4 h, indicating the presence of a kinetic barrier for PMAS to form a compact structure with multiple binding sites on QD surfaces. Note that the original QDs were not soluble in pure DMSO. The DMSO solubility of QDs after the first ligand exchange at 50 °C indicates that the QDs should be coated with a mixture of the original hydrophobic ligands and the loosely attached PMAS ligand. These QDs were soluble in water and buffer solutions; however, the solution was unstable, and the QDs formed aggregates within 24 h. In our previous study, the use of hyperbranched polyethylenimine in ligand exchange reactions did not show this kind of kinetic barrier.[30] The difference between these two systems could be due to the spherical configuration and highly dense functionality in hyperbranched polymers that are more favorable for binding with QD surfaces than linear

(30) Duan, H. W.; Nie, S. M. *J. Am. Chem. Soc.* **2006**, *129*, 3333–3338.

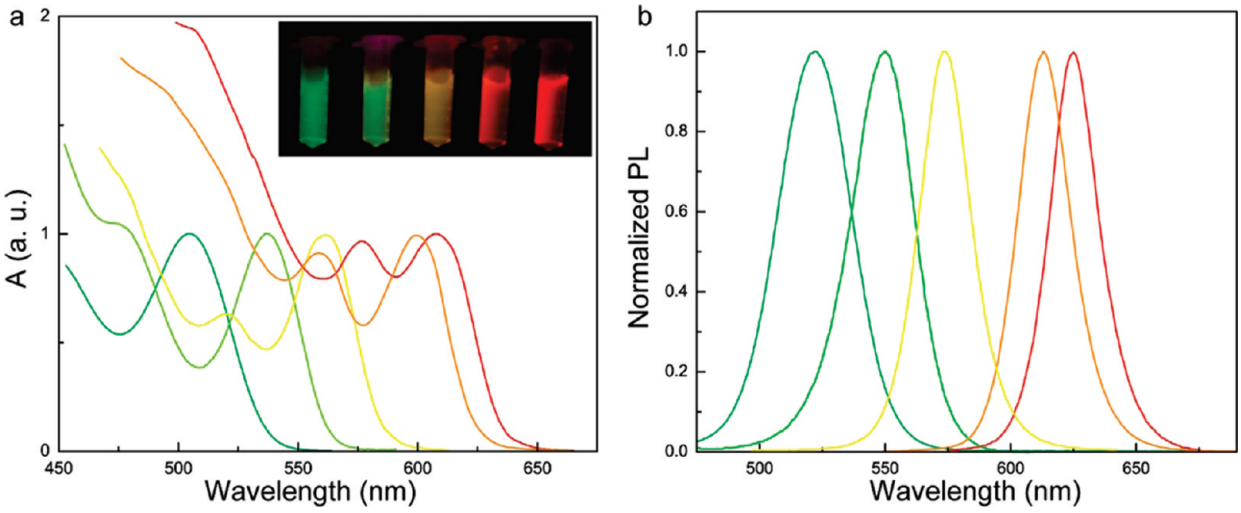

Figure 4. UV−vis (a) and photoluminescence spectra (b) of a series of core−shell QDs (CdSe/ZnS or CdSe/CdS/ZnS) coated with multivalent PMAS ligands in water (Inset in a: photos of QDs under 365 nm UV irradiation).

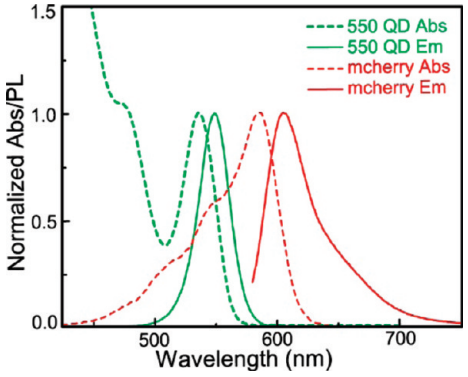

Figure 5. Spectroscopic properties of the 550 nm QD donor and the mCherry acceptor: QD (green line), mCherry (red line), absorption spectra (dash line), and emission spectra (solid line).

PMAS ligands. The oligo-PEG is introduced for a better colloidal stability and reducing nonspecific binding. The QDs with the oligo-PEG modification showed excellent colloidal stability in a large pH range (pH 5−12). A previous report by Ting et al. showed that oligo-PEG with less than eight repeating units does not affecting the metal-affinity binding of HIS-tag and QD surfaces.[31]

In negatively stained images from transmission electron microscope (TEM), PMAS coated 6.0 nm QDs (QD@PMAS) form a closely attached monolayer (Figure 2a), and the polymer ligand layer is barely visible. To directly compare QD@PMAS with QD probes encapsulated with amphiphilic copolymers, the same QDs were also coated with the copolymer of maleic anhydride and octadecene (PMO). The TEM image (Figure 2b) shows that the amphiphilic PMO coating leads to a coating layer of ~3 nm in PMO coated QDs (QD@PMO), suggesting the compactness of the PMAS coating. Currently, amphiphilic copolymers containing the maleic anhydride component are widely employed to prepare water-soluble nanocrystals including QDs, taking advantage of the hydrophobic interaction between the hydrophobic monomers, that is, octadecene, and the capping ligand on QDs.[11−13] It is obvious that the hydrophobic layer contributes to the size increase in QD@PMO (Figure 3). The compactness of QD@PMAS is also supported by dynamic light scattering (DLS) measurements (Table 1), which show that QD@PMAS and QD@PMO have average hydrodynamic diameters of 9.0 nm and 14.0 nm, respectively, leading to a coating thickness of 1.5 nm for PMAS and 4.0 nm for PMO. As expected, the coating thickness in solution is slightly larger than those obtained from TEM in the dry state. The coating thickness is consistent for different sized QDs. For 4.2 nm QDs, DLS measurements show a coating thickness of 1.6 nm and 3.5 nm for PMAS and PMO, respectively. Figure 2c shows that QD@PMAS migrates faster than QD@PMO in a 1% agarose gel, again resulting from their compact sizes. Similarly, due to both increased sizes and reduced charges by PEG grafting, QD@PMO with PEG (MW ≈ 5000 Da) grafts exhibit even lower electrophoretic mobility than QD@PMO. In addition, the presence of about 10% Ni-NTA on the QD@PMO surface did not lead to significant changes in their zeta potentials (−30 mV) and gel shifts. Figure 4 displays the UV−vis and photoluminescence spectra of five QD@PMAS with the emission maximum from 525 to 620 nm. QD@PMAS shows stable fluorescence with high QY (30−45%) and negligible peak shifts (< 2 nm) compared to the parent QDs. The QDs are very stable at ambient conditions, and no obvious change in sizes and gel migration were observed after three months of storage. Also, continuous UV irradiation (365 nm) for 3 h did not alter their absorption and fluorescence profiles as well as quantum yields.

Self-Assembled QD-mCherry Conjugates for FRET. QDs are increasingly used for FRET designs due to their unique properties such as tunable narrow emission, large Stokes shifts, and sufficient surface areas for multiplexed FRET configuration.[4,26,32,33] Here, 550 nm QDs and

(31) Liu, W. H.; Howarth, M.; Greytak, A. B.; Zheng, Y.; Nocera, D. G.; Ting, A. T.; Bawendi, M. G. *J. Am. Chem. Soc.* **2008**, *130*, 1274–1284.
(32) Boeneman, K.; Mei, B. C.; Dennis, A. M.; Bao, G.; Deschamps, J. R.; Mattoussi, H.; Medintz., I. L. *J. Am. Chem. Soc.* **2009**, *131*, 3828–3829.
(33) Dennis, A. M.; Bao, G. *Nano Lett.* **2008**, *5*, 1439–1445.

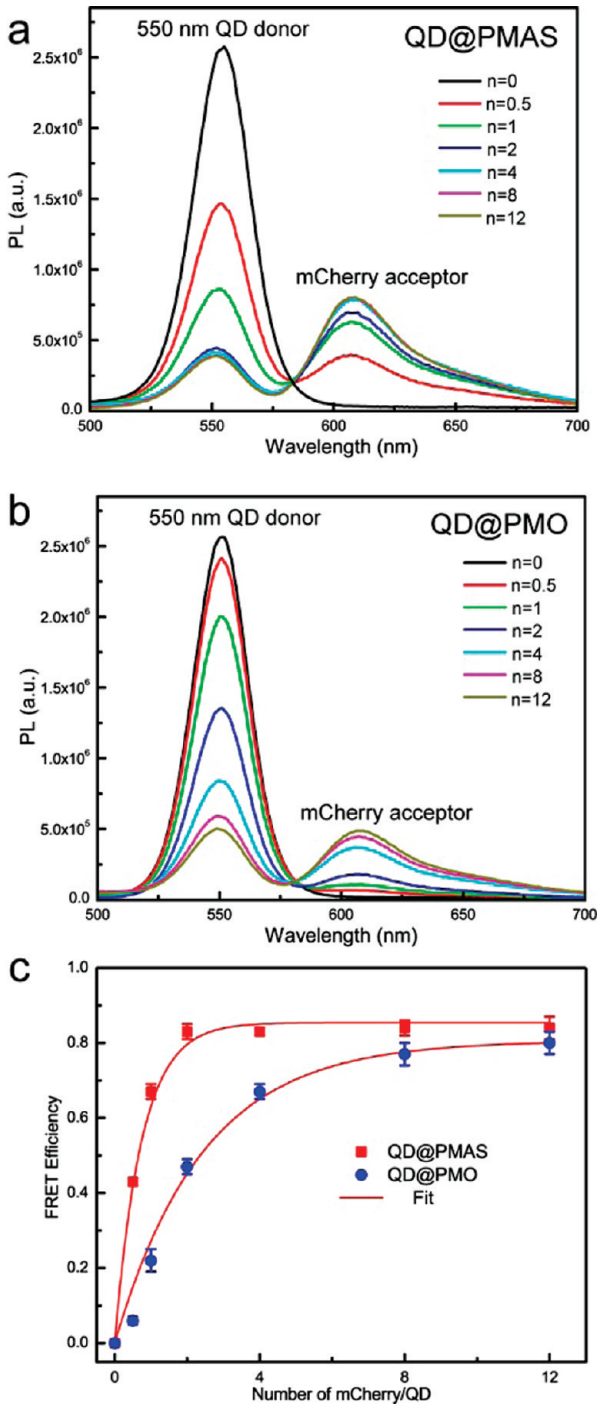

Figure 6. FRET experimental data of the QD-mCherry construct. Representative photoluminescence spectra of QD-mCherry conjugates with increasing mCherry/QD ratios: QD-PMAS (a) and QD-PMO (b). (c) Plots of FRET efficiency obtained from the QD photoluminescence loss as in (a) and (b).

mCherry (MW = 28.8 kDa, ε_{587} = 72 000 $M^{-1}cm^{-1}$, QY = 22%) were selected as a donor−acceptor pair because of their optimal spectral overlapping (Figure 5), indicated by the large overlap integral ($J = 3.5 \times 10^{-13}$ $cm^6 \cdot mmol^{-1}$) obtained from FRET calculation. This FRET pair has a Förster distance (R_0) of 5.0 nm for QD@PMAS (QY = 30%) and 5.2 nm for QD@PMO (QY = 35%).

As shown in Figure 6, it is clear that mCherry with a His-tag is able to assemble on QD@PMAS and leads to a progressive loss of QD fluorescence and an increase of sensitized mCherry emission with increasing mCherry/QD ratios (n) for $n \leq 4$. FRET efficiency was calculated using eq 2, showing 67% FRET efficiency at 1 acceptor per QD and 82% at a ratio of 2 mCherry per QD. Our previous work has shown that the Ni-NTA functionality allows for strong binding of antibodies with His-tag on the surface of QD@PMO.[34] For a direct comparison of the FRET efficiency, the amphiphilic PMO copolymer was functionalized with Ni-NTA (Figure 3) for mCherry binding. It is consistent that the obtained QD probes also can bind mCherry with a His-tag, leading to FRET efficiency of 22% and 47% at QD:mCherry ratios of 1:1 and 1:2, respectively. Figure 6c summarizes the corresponding FRET efficiency (derived from the QD fluorescence loss) as a function of the QD:mCherry ratios. FRET efficiency is extremely sensitive to the distance between fluorescence donor and acceptor (eq 3). We believe that the highly efficient FRET of QD@PMAS−mCherry in comparison with the QD@PMO system is a result of the compact PMAS coating, which brings the QD donor and mCherry acceptor closer in distance. According to eq 3, the efficiencies at $n = 1$ result in a center-to-center separating distance of QD and mCherry of 4.4 nm for QD@PMAS and 6.4 nm for QD@PMO. Although the detailed configuration of the two QD-mCherry conjugates needs further investigation, it can be expected that the bulky PMO coating contributes to the major part of this difference of 2.0 nm (Figure 7), as shown in TEM and DLS measurements. No further change in fluorescence spectra has been observed for QD@PMAS−mCherry at $n > 4$, indicating the saturation of mCherry binding on QD surfaces. Similar saturation was not available when QD@PMO was used as the scaffold for mCherry, and continuous loss of QD PL was observed up to $n = 12$. This could be due to the large surface area of QD@PMO (2.4 times of that of QD@PMAS based on hydrodynamic sizes), therefore being able to accommodate more acceptors. This reproducible saturated binding provides a possible approach to control the valency of bioaffinity ligands on these small QDs, which has been a major challenge in QD bioconjugation. Gel electrophoresis results (Figure 7c,d) also show the same trends of saturation: the binding of up to four copies of mCherry on QDs gradually slows down their migration in agarose gel due to the increased sizes; further increase of mCherry concentration did not show any impact. For the bulkier QD@PMO, protein binding leads to a smaller change in gel mobility due to the minor relative increase in sizes. Gel fluorescence images taken by a two-filter system: SYBR Green filter for 550 nm QD and ethidium bromide filter for mCherry, showed that excitation at 365 nm resulted in the red emission of mCherry due to energy transfer from QDs, further confirming the FRET between QDs and mCherry. The two series of conjugates all showed

(34) Yang, L.; Mao, H.; Wang, Y. A.; Cao, Z. H.; Peng, X. H.; Wang, X. X.; Duan, H. W.; Ni, C. C.; Yuan, Q. A.; Adams, G.; Smith, M. Q.; Wood, W. C.; Gao, X. H.; Nie, S. M. *Small* **2009**, *5*, 235–243.

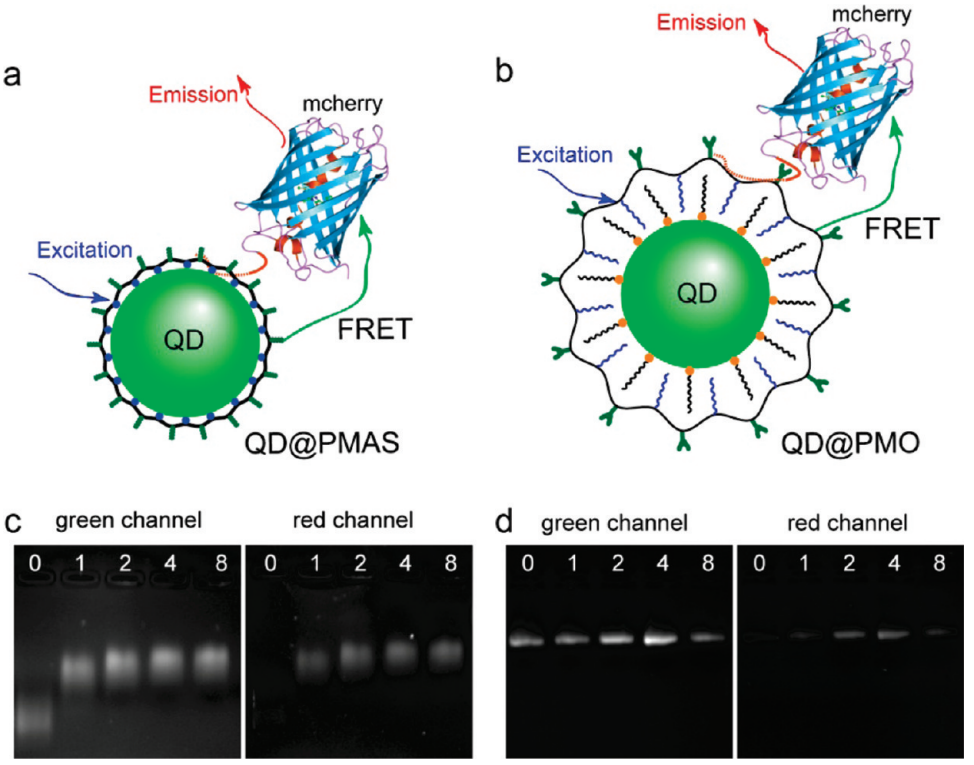

Figure 7. Schematic diagrams of FRET pairs based on QD with PMAS (a) and PMO (b) coatings. Electrophoretic migration of mCherry conjugates of QD@PMAS (c) and QD@PMO (d) with increasing mCherry/QD ratios.

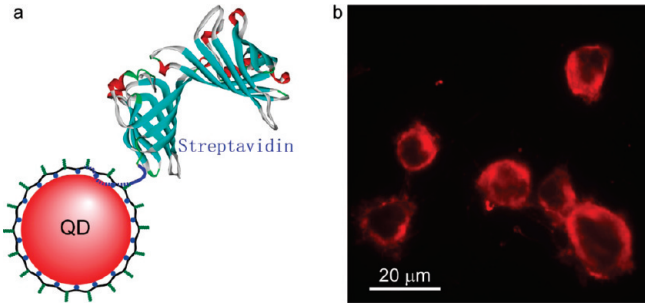

Figure 8. (a) Schematic illustration of the conjugate of His-tag streptavidin and QD-PMAS. (b) MDA-MB-231 breast cancer cells stained with philloidin-biotin and QD-streptavidin conjugates.

the same emission pattern for both green QDs and red fluorescence from mCherry, proving their coexistence in the conjugates. The different emission colors of these QD-mCherry conjugates under UV irradiation (365 nm) can be easily distinguished with the naked eye: all of the QD@PMAS exhibits red color at $N \geq 1$, whereas QD@PMO shows a change of color from green, yellow, and orange to red when N increases gradually.

Self-Assembled Conjugates of QD and His-Tagged Streptavidin for Immunofluorescence Staining. One of the challenges to construct biconjugated QDs is to maintain the affinity of bioligands after being conjugated with QDs. Figure 8 shows that 610 nm QDs with His-tagged streptavidin kept their recognition ability and can be used to label actin prestained with biotinylated phalloidin in MDA-MB-231 breast cancer cells. Control QDs without streptavidin underwent the same treatment and exhibited little staining. Previous studies by Mattoussi et al. reported that the binding constant of His-tag with the QD surface is about 1 nM,[35] indicating the QD@PMAS with His-tagged bioaffinity ligands is robust and potentially can be used in varieties of applications requiring harsh treatment. This self-assembled approach to preparing bioaffinity QDs offers more unique advantages than chemical conjugation. It is possible to genetically engineer antibodies for site-specific His-tag modification to ensure conformation favorable binding and avoid loss of activity of the ligand. This could avoid problems such as cross-linking-induced particle aggregation and blocking of active binding sites of bioaffnity ligands happening in chemical conjugation.

Conclusions

In summary, we have reported a new type of multivalent polymer ligands to prepare highly stable hydrophilic QDs with compact sizes. The combination of these highly stable QDs and readily available recombinant His-tagged proteins offers new possibilities to design a new generation of QD probes with compact sizes for FRET-based biodetection assays and intracellular imaging applications. It can be expected that the multifunctional polymer ligands with multiple thiol and carboxylic acid groups will also find uses for metal and metal oxide nanostructures.

Acknowledgment. HD acknowledges the program of Nanyang Assistant Professorship for generous financial support.

(35) Sapsford, K. E.; Pons, T.; Medintz, I. L.; Higashiya, S.; Brunel, F. M.; Dawson, P. E.; Mattoussi, H. *J. Phys. Chem. C* **2007**, *111*, 11528–11538.